Int. J. Electrochem. Sci., 9 **(2014)** 7431 - 7445

International Journal of
ELECTROCHEMICAL
SCIENCE
www.electrochemsci.org

Structural characterization of (E)-4-((4-nitrobenzylidene)amino)phenol Schiff Base. Investigation of its Electrochemical, Cytotoxic, Antibacterial, and Antifungal Activity

V.M. Jiménez-Pérez[1], *B.M. Muñoz-Flores*[1,*], *L.M. Blanco Jerez*[1,*], *A. Gómez*[1], *L. D. Rangel*[1], *R. Chan-Navarro*[1], *N.Waksman*[2], *R. Ramírez-Durón*[2]

[1]Universidad Autónoma de Nuevo León, Facultad de Ciencias Químicas, Ciudad Universitaria, Av. Universidad s/n. C. P. 66451, Nuevo León, México.
[2] Universidad Autónoma de Nuevo León, Facultad de Medicina, Ciudad Universitaria, Av. Universidad s/n. C. P. 66451, Nuevo León, México.
[*]E-mail: leonyjerez@gmail.com; bmunflo@yahoo.com.mx

Received: 11 August 2014 / *Accepted:* 2 October 2014 / *Published:* 28 October 2014

Reaction of 4-hydroxybenzaldehyde with aminophenol provided the (*E*)-4-((4-nitrobenzylidene)amino)phenol, which was characterized by NMR, IR, X-ray diffraction and voltammetry techniques. The Schiff base crystalizes in the monoclinic system, space group *P*21/*c*, where the crystal structure shows a usual *trans*-configuration with respect to the C=N double bond. From the electrochemical study the redox processes of this compound were established. The electrogeneration potential of the imine group dianion was also determined. Knowing the electrogeneration potential of the imine group dianion radical will allow obtaining coordination compounds of this radical with metals whose cations are generated from sacrificial anodes in an electrochemical cell. According to biological activity studies, title compound has potential as cytotoxic, antibacterial and antifungal agent.

Keywords: Schiff base, cyclic voltammetry, cytotoxicity, antibacterial, antifungal.

1. INTRODUCTION

More than one hundred and fifty years the Schiff bases are still an important class of organic compounds in chemical, medical and pharmaceutical areas. Schiff bases have shown a wide range of biological activities, such as antipyretic [1], antimalarial [2], antiproliferative [3], antiviral [4], antitumor [5], antioxidant [6], antibacterial [7], and antifungal [8]. Recently, the hydroxy-substituted Schiff bases have received considerable attention due to good anticancer activity; for example, Lui *et*

al. report a new Schiff base (*N*-(3,4-dihydroxybenzylidene)ferroceneamine, (Scheme 1, **I**) with an excellent biological activity against the HeLa cancer cell line, where the *o*-dihydroxy groups play an important role [9]. Also, Zhou *et al.* carried out the synthesis of several hydroxy-substituted Schiff bases and found good cytotoxicity to HepG2 cancer cells (Scheme 1, molecule **II**) [10]. In this context, we are interested in the synthesis, electrochemical characterization and cytotoxic activity of organic compounds [11, 12].

In addition, several researchers have suggested that there is a direct correlation between the redox potentials of Schiff bases, and their complexes, and their ability to behave as oxygen carriers [13]. For this reason, in recent years there has been much interest in determining the electrochemical characteristics of Schiff bases and their metallic complexes in order to establish the relationship between these redox potentials and the ligand structure [14]. In this paper we applied the potential sweep techniques to study the electrochemical behavior of the referred Schiff base. In particular, our interest was to determine the dianion radical formation potential associated to the reduction process of Schiff base imine group. In this paper we report the crystal structure, the chemical/electrochemical characterization, the cytotoxicity *in vitro*, and the antibacterial and antifungal activity of (*E*)-4-((4-nitrobenzylidene)amino)phenol (Scheme 1, Compound **1**). Benzalaniline (Compound **2**) was also studied for electrochemical comparison.

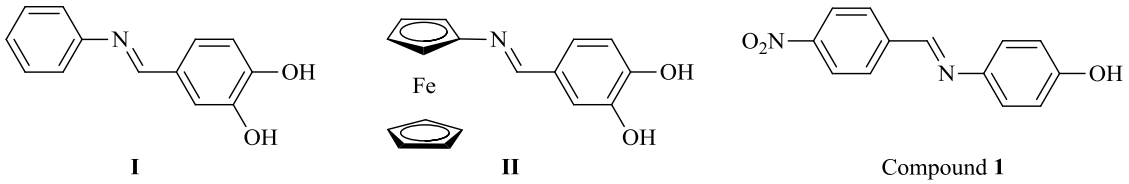

Scheme 1. Schiff bases with cytotoxic activity.

2. EXPERIMENTAL

2.1. General remarks

All starting materials were purchased from Aldrich Chemical Company. Solvents were used without further purification. The melting points for Compound **1** and Compound **2** were determined on an Electrothermal Mel-Temp apparatus and were not corrected. Infrared spectra were recorded using a Bruker Tensor 27 FT-IR spectrophotometer equipped with a Pike Miracle™ ATR accessory with a single reflection ZnSe ATR crystal. UV spectra were obtained with a Shimadzu 2401PC UV/VIS spectrophotometer. High resolution mass spectra were acquired by liquid chromatography mass LC/MSD TOF on an Agilent Technologies instrument with APCI (Atmospheric Pressure Chemical Ionization) as ionization source. ^{1}H and ^{13}C spectra were recorded in dimnethylsulfoxide-d_6 on a Bruker Advance DPX 400. Chemical shifts (ppm) are relative to $(CH_3)_4Si$ for ^{1}H and ^{13}C.

2.2. X-ray crystallography

The single crystals of Compound **1** suitable for X-ray structural studies were obtained by slow evaporation from mixtures of CH_2Cl_2 and hexane. The crystal data were recorded on an Enraf Nonius Kappa-CCD (k Mo Ka = 0.71073Å, graphite monochromatic, T = 293 K, CCD rotating images scan mode). The crystals were mounted on a Lindeman tube. Absorption corrections were performed using the SHELX-A program [15]. All reflection datasets were corrected for Lorentz and polarization effects. The first structure solution was obtained using the SHELXS-97 program, and then the SHELXL-97 program was applied for refining and delivering data. All software processing was done in the WIN-GX environment program set [16]. Molecular perspectives were created using the ORTEP3 drawing application [17]. All the heavier atoms were found by Fourier map difference and refined anisotropically. Some hydrogen atoms were found by Fourier map differences and refined isotropically. The remaining hydrogen atoms were geometrically modeled and were not refined.

2.3. Electrochemical studies

All the electrochemical measurements were carried out in a PGSTAT 30 AUTOLAB potentiostat/galvanostat. The voltammetric experiments were carried out under a nitrogen atmosphere using the typical three-electrode configuration: a glassy carbon disk as working electrode, a platinum bar as auxiliary electrode (both from BAS), and a silver wire with redox Fc/Fc+ couple as pseudo-reference electrode. The redox couple was externally calibrated with 4.0 mM Fc/Fc+ and 0.1 M TBAHFB solutions in acetonitrile. The redox processes were determined by cyclic voltammetry (CV). Differential pulse voltammetry (DPV) was used to obtain a better definition of the reduction processes. In order to determine the substituent effects on the absorption band positions, the spectroscopic UV-Vis measurements were obtained in a 100Conc VARIAN Cary spectrophotometer.

2.4. In vitro cytotoxicic assay

Human lymphoblastic leukemia MOLT-4 cells were employed to test cytotoxic effects of Compound **1**. MOLT-4 cells were maintained in RPMI media supplemented with 10% Foetal Bovine Serum (Gibco), 100 IU/mL penicillin and 100 µg/mL streptomycin. Cell line culture was carried out at 37°C in an Incubator (Shell Lab, TC-2323) with a 95% air and 5% CO_2 atmosphere. Cytotoxicity of Compound **1** was tested at 0.5, 1.0, 2.0, 5.0, 8.0, 10, 20 and 50 ppm. Leukemia cells were seeded in 24-well tissue culture plates with $5x10^4$ cells/well and immediately after platting they were supplied with Compound **1** in triplicate. All dilutions were prepared with fresh culture media and plates were incubated for 24 hours. Microscopic analysis was carried on to explore for morphological changes in cells. Surviving cells were measured by the MTS method [3-(4,5-dimethylthiazol-2-yl)-5-(3-carboxymethoxyphenyl)-2-(4-sulfophenyl)-2H-tetrazolium] and related to the mock cell population by measuring absorbance at 590 nm to establish cell viability.

2.5. Antibacterial assays

Radial diffusion assays (RDA) were performed using a bacteria density of 0.6 O.D. units for *Salmonella typhimurium* (ATCC 14028). Assays were carried out in 100 x 15 mm Petri dishes poured with 20 ml nutrient agar media and inoculated with the bacterial strain. Two 25 μL aliquots of Compound **1** aqueous solutions (100 and 50 ppm) were dropped in the middle of each dish. All preparations were incubated for 24 hours at 37 °C. Once incubation time elapsed, growing inhibition areas were measured to establish the antibacterial effect of Compound **1**.

2.6. Antifungal assays

Fungus growing inhibition capability of Compound **1** was probed against two filamentous fungi. *Penicillium sp.* and *Aspergillus niger* were seeded separately in sterilized Potato Dextrosa Agar medium (PDA) in a 24-well plate through 10 μL spores suspension. Compound **1** solution of 250, 125, 50, 25 y 5 ppm were added to culture wells and incubated for 5 days at 28ºC. After incubation time elapsed, the culture wells were visually examined. The lack of irregular dark dusty zones as a result of sporulation process was considered as an indication of mycelium growing inhibition.

2.7. Chemical synthesis

*(E)-4-((4-nitrobenzylidene)amino)phenol (Compound **1**)*

Compound **1** has been already reported [18] but has not been characterized. A solution of 4-nitrobenzaldehyde (0.5 g, 3.3 mmol) and 4-aminobenzoic acid (0.41 g, 3.3 mmol) in benzene (30 mL) was heated under reflux for 6 h, with a Dean-Stark apparatus used for the azeotropic removal of water, and then allowed to cool to room temperature. Removal of solvent yielded an orange solid, which was recrystallized from hot benzene (10 mL). Yield: 0.61 g 77%. M. p. 168 ^{o}C. ^{1}H NMR (400.13 MHz, DMSO-d_6, 25 ^{o}C) δ : 6.86 (d, ^{3}J = 8.8 Hz, 2H, H-9/H-13), 7.33 (d, ^{3}J = 8.8 Hz, 2H, H-10/H-12), 8.12 (d, ^{3}J = 8.8 Hz, 2H, H-6/H-2), 8.33 (d, ^{3}J = 78.4 Hz, 2H, H-5/H-3), 8.79 (s, 1H, H-7), 9.76 (bs, 1H, OH). ^{13}C {^{1}H} NMR (100 MHz, DMSO-d_6, 25 ^{o}C) δ : 115 (C9/C13), 123.1 (C10/C12), 123.9 (C3/C5), 129.0 (C2/C6), 141.6 (C8), 142 (C4), 148 (C1), 154.6 (C7), 157.2 (C11). COSY correlation [δ_H/δ_H]: 6.86/7.33 (H-9 and H-13/H10 and H-12), 8.12/8.33 (H-6 and H-2/H5 and H-3). HSQC correlation [δ_H/δ_C]: 6.86/115 (H9/C9), 7.33 (H10/C10), 8.12/129.0 (H6/C6), 8.33/123.9 (H5/C5), 8.79/154.6 (H-7/C7). HMBC [δ_H/δ_C]: 6.86/141.6 (H-9/C8), 8.12/148 (H-6/C1), 8.33/142 (H-5/C4), 7.33/157.2 (H-10/C11). IR$_{\upsilon max}$ (ATR): 3440 (b, -OH), 2837 (m, =C-H), 1624 (m, C=N), 1577 (m, C=C), 1505 and 1337 (s, NO_2), 1261.3 (C-N), 1169 (m, C-O), 849.6, 831.4, 748.8, 718.9, 688.5, 672.8 cm^{-1}. TOF-MS calc. for [($C_{13}H_{11}N_2O_3$+H)$^{+}$]: 243.076418 u.m.a; Exp.: 243.076334 u.m.a (Error = - 0.348844 ppm).

*Benzalaniline (Compound **2**)*

Compound **2** was prepared for electrochemical comparison. A solution of benzaldehyde (0.5 g, 4.7 mmol) and aniline (0.43 g, 4.7 mmol) in benzene (30 mL) was heated under reflux for 24 h, with a Dean-Stark apparatus used for the azeotropic removal of water, and then allowed to cool to room temperature. Removal of solvent yielded a colorless solid, which was recrystallized from CH_2Cl_2/hexane (2:8). Yield: 0.81 g (92 %). M. p. 41^oC. $IR_{\upsilon max}$ (ATR): 3060, 2891, 1625, 1591, 1577.6, 1483.1, 1450.4 cm^{-1}.

3. RESULTS AND DISCUSSION

The condensation reaction of 4-hydroxybenzaldehyde with aminophenol provided the Compound **1** with good yields (Scheme 2), as an orange crystalline material with good solubility in common organic solvents. Compound **1** has been already reported, but its crystal structure is unknown.

3.1. Spectroscopic and spectrometric characterization

The ^1H NMR spectra of Compound **1** show two signals at high frequencies (9.76 and 8.79 ppm), corresponding to the hydroxy and imino group, respectively. In addition, two AB systems of the aromatic rings protons lie in the δ range of 6.8-8.4 ppm. The identification of ^{13}C data of the Schiff base was based on HSQC experiment results: the spectrum exhibits correlations of H-9 (6.86 ppm) with C-9 (115 ppm), and H-10 (7.33 ppm) with C-10 (123.1 ppm). Furthermore, the experiment indicated a correlation between H-5 (8.33 ppm) and a chemical shift at 123.9 ppm, which corresponds to C-5 (see the Appendix). The ^{13}C NMR data show that the signal of the imino group (C7) appears at 154.6 ppm, in agreement with data reported for analogous Schiff bases [19]. In order to make an unambiguous assignment of quaternary carbon atoms C4, C1, C8 and C11, the heteronuclear multiple bond correlation (HMBC) experiment was performed. The HMBC spectrum shows two important correlations: H-10 with δ at higher frequencies in 157.2 ppm to C11, and H-9 with the 141.6 ppm to C-8 (see supporting information). IR spectral analysis showed stretching bands at 3440 and 2837 cm^{-1}, which are assigned to the O-H and C-H bonds. The strong band at 1624 cm^{-1} was assigned to the C=N bond. Also, the symmetric and asymmetric stretching vibrations of NO_2 occur at 1505 and 1337 cm^{-1}. The high resolution mass spectra (HRMS) of compound **1** showed the base peak corresponding to the molecular ion.

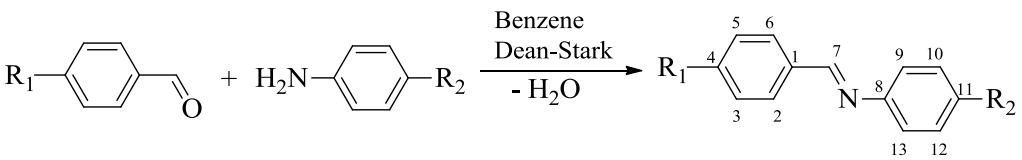

1: $R_1 = NO_2$, $R_2 = OH$ (77 %)
2: $R_1 = H$, $R_2 = H$ (92 %)

Scheme 2. Synthesis of Schiff bases **1** and **2**.

3.2. X-ray analysis

The structure of Compound **1** is represented by the thermal ellipsoid plot in Fig. 1 and corresponds to the monoclinic space group *P*21/*c* (Table 1). The aromatic rings are not in the same plane; the dihedral angle between mean planes is 15.59° (Fig. 1). The N1-C7 [1.271(3) Å] bond length for the Schiff base is almost the same as that of a similar organic compound reported by our group (1.272(3) Å) [20]. The azomethine group is in the same plane as the nitro ring, probably because of the close contact between C(2)-H(2) and N(1) 2.623(4) Å, [∠ C-H···N: 97.73°]. A molecule of ethanol is present in the asymmetric unit cell. This molecule causes the formation of an infinite polymer because of the bond of its hydrogen with the imino nitrogen (OH···N=C 2.071(3) Å, ∠ O-H-N 170.67(5)) (see the Appendix). Through π-π interactions as offset face to face the crystal structure show an infinite 2D network (Fig. 2).

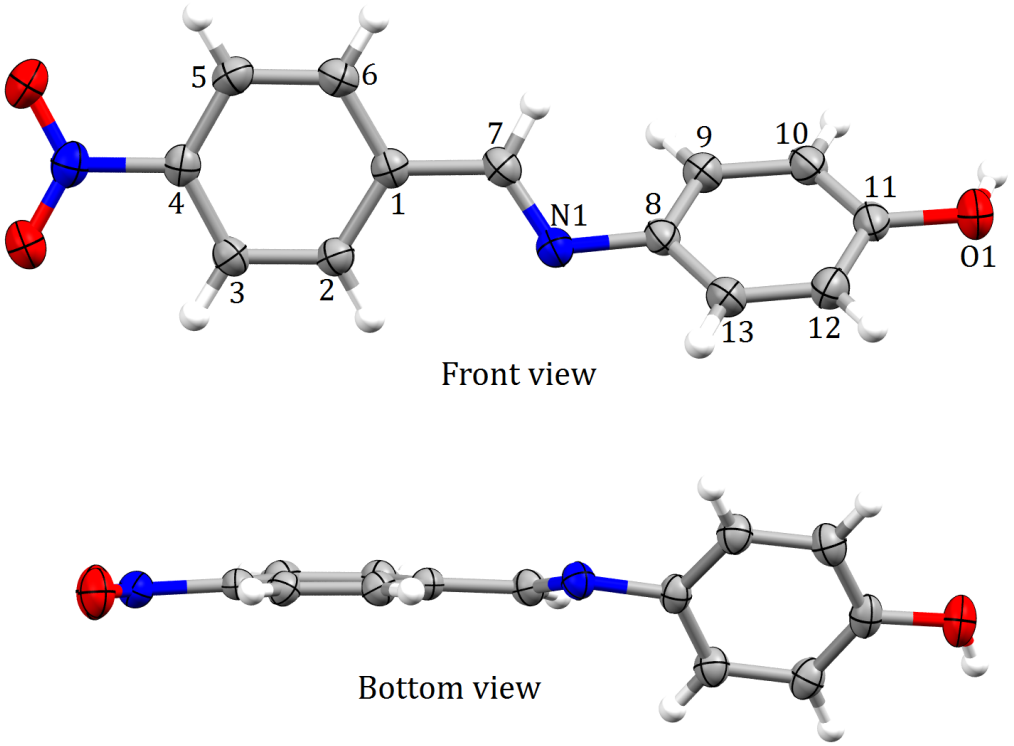

Figure 1. Molecular structure of **1**. The anisotropic displacement parameters are depicted at the 30% probability level. Hydrogens were omitted for clarity. Selected bond lengths: C7-N1 1.271(3), C4-N 1.478(3), C11-O1 1.362(4), C1-C7 1.469(3), and N1-C8 1.426(3) Å.

Table 1. Crystalline structure data and structure refinement for the title compound.

	1
Empirical formula	$C_{13}H_{10}N_2O_3$
Formula weight	242.23

Temperature, K	293(2)
Wavelength	0.71073
Crystal system	Monoclinic
Space group	*P*2(1)/*c*
a, Å	13.3904(3)
b, Å	6.8555(2)
c, Å	17.1294(5)
α	90.00 ^{o}
β	112.6310(10)^{o}
γ	90.00^{o}
V,Å^{3}	1451.37(7)
Z	5
$\rho_{calc,mg.cm}^{-3}$	1.306
μ, mm^{-1}	0.094
2θ range for data collection	2.47 – 27.49°
Index ranges	-17 ≤ *h* ≤ 17 -21 ≤ *k* ≤ 21, -12 ≤ *l* ≤ 12
	-8 ≤ *k* ≤ 8
	-22 ≤ *l* ≤ 19
No. of reflns collected	13738
No. of indep reflns	3261
[R_{int}]	0.0562
Fit goodness	1.188
R_1, wR_2 (I>2σ(I))	0.0562/0.1504 0.1318
*R*1, w*R*2 (all data)	0.0877/0.1687 0.1387

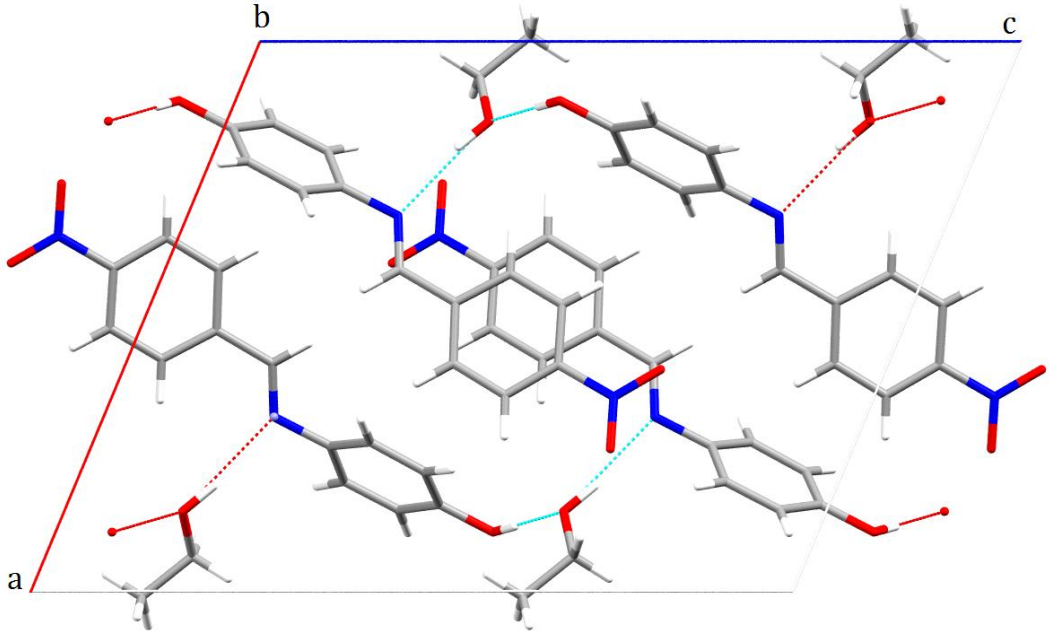

Figure 2. Part of the crystal structure [21], showing the polymeric structure growing along the ***b*** cell axis.

3.3. Electrochemical study

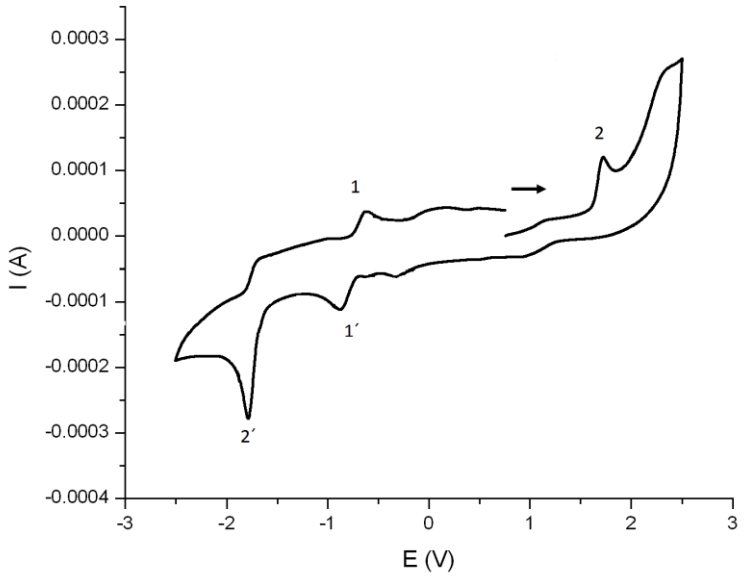

Figure 3. Cyclic voltammetry of Compound **2** in ACN with TBAHFB at 100 mV/s with a carbon disk electrode (E vs. Fc/Fc^{+}); the arrow indicates the sweep direction.

The structural difference between Compound **1** and **2** is the presence of nitro and hydroxy groups in the Compound **1**. The comparison of their CVs gave us information about the

electrochemical behavior of the imine group in both systems. The Compound **2** CV result is an evidence of the imine group electrochemical activity, which includes two reductions and two oxidation processes (Fig. 3).

Table 2 shows the peak anodic and cathodic potentials, which are associated to oxidation and reduction processes of the imine group. In particular, the reduction process 2´ at -2.11 V vs $E_{Fc/Fc+}$ refers to the formation of a dianion radical of the imine group because this is the only organic group that can be reduced. Knowing the electrogeneration potential of the dianion radical will allow obtaining coordination compounds with metals whose cations are generated from sacrificial anodes. This process takes place in an electrolytical cell that operates at a controlled potential (equal to the dianion radical formation potential). The process allows the *in situ* chemical metallation of the ligand corresponding to this dianion with the electroformed cations [22-24].

Table 2. Compound **2** redox potentials from CV.

Compound/Ep (V)	**Epa_1(1)**	**Epa_2(2)**	**Epc_1(1)**	**Epc_2(2)**
2	-0.62	1.71	-1.23	-2.11

The application of the DPV technique allowed us determining the nature of the associated reduction processes in Compound **2**. Fig. 4 shows the resulting voltammogram at 100 mV/s, which reveals the presence of two reduction processes: one process at -0.8 V, and the other process at -2.09 V, associated to the anion and dianion radicals formation, respectively.

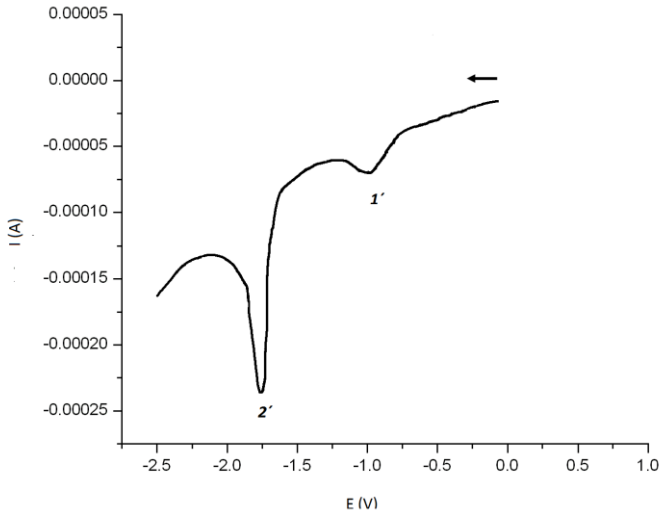

Figure 4. Differential pulse voltammetry of Compound **2** in ACN with TBAHFB at 100 mV/s with a carbon disk electrode (E vs. Fc/Fc^+); the arrow indicates the sweep direction.

Fig. 5 shows the CV of Compound **1** in the same conditions as for Compound **2** (shown in Fig. 3). This voltammogram shows three reduction and three oxidation processes. The oxidation processes

A, B and C take place at E_{pa1} = -0.93 V, E_{pa2} = -0.70 V and E_{pa3} = 0.19 V, respectively; the reduction processes a, b and c take place at E_{pc1} = -1.33 V, E_{pc2} = -1.92 V and E_{pc3} = -1.16 V, respectively. Comparison of **1** and **2** reduction processes shows that two reduction processes can be associated to the activity of the imine group.

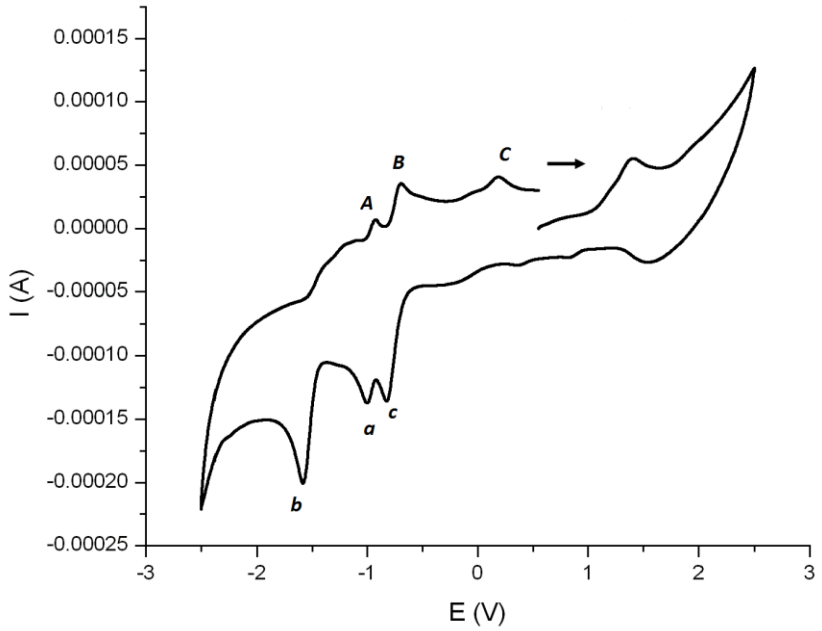

Figure 5. Cyclic voltammetry of **Compound 1** in ACN with TBAHFB at 100 mV/s with a carbon disk electrode (E vs. Fc/Fc^+); the arrow indicates the sweep direction.

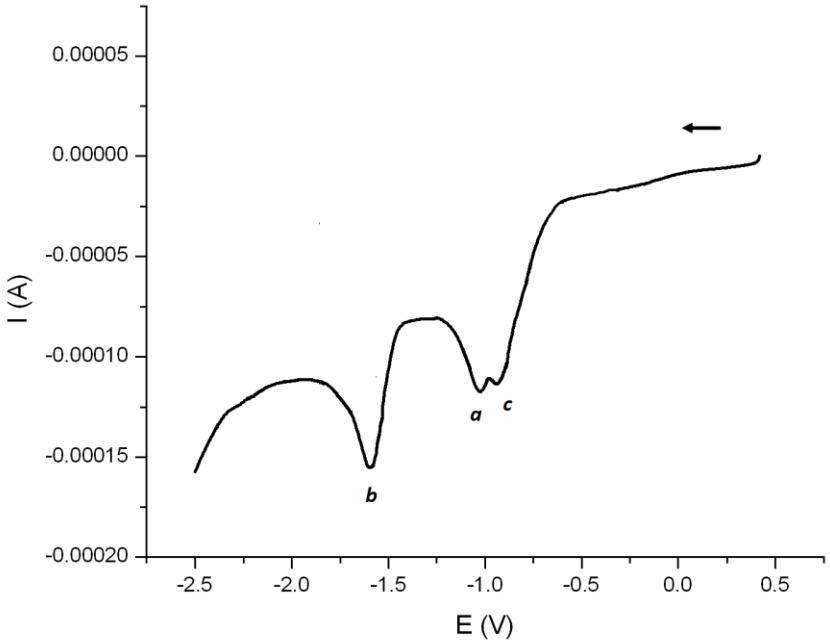

Figure 6. Differential pulse voltammetry of **Compound 1** in ACN with TBAHFB at 100 mV/s with a carbon disk electrode (E vs. Fc/Fc^+); the arrow indicates the sweep direction.

This result means that the process of the dianion radical formation in **1** could be process b at -1.92 V. In this case, the effect of the OH^- and NO_2 substituent groups cause a shift to more positive potentials than those obtained for Compound **2**.

Fig. 6 shows the result of applying the DPV technique to the Compound **1** molecule to more precisely determine the dianion radical formation potential. Comparing the voltammograms of Fig. 6 and Fig. 4, we conclude that the formation potential of Compound **1** dianion radical is -1.92 V. This value is slightly different from that obtained for the Compound **2** because of the effect of substituent groups.

To determine the effect of the type of supporting electrolyte on the dianion radical formation potential, the CV of Compound **1** was also carried out in the presence of tetrabuthylammonium hexafluorophosphate (TBAHFP). In this case, the dianion radical formation potential was -1.95 V, a more negative value than the -1.92 V obtained for TBAHFP (Fig. 7). This result shows that TBAHFB is a better supporting electrolyte because it favors the thermodynamic process leading to the dianion radical formation.

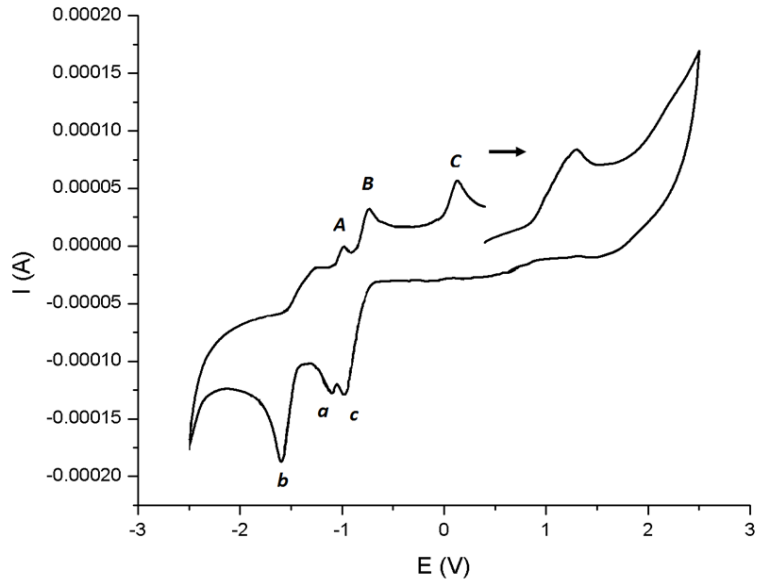

Figure 7. Cyclic voltammetry of Compound **1** in ACN with TBAHFP at 100 mV/s with a carbon disk electrode (E vs. Fc/Fc^+); the arrow indicates the sweep direction.

Finally, a comparative study using the spectroscopic UV-Vis technique was carried out for Compound **2** and **1** to determine the effect of hydroxyl and nitro groups on the UV absorption spectra of these Schiff base compounds. Figures 8 and 9 show these spectra. The absorption spectra of the Compound **2** (Fig. 8) shows only one main peak at 262 nm due to π-π* of the imine group electronic transitions thought the molecule. This result clearly shows that this material absorbs mainly in the ultraviolet region. The absorption spectra for Compound **1** (Fig. 9) revealed that the presence of nitro group in the *para* position of the aromatic ring causes a red-shift of the imine group band from 262 to 373. In addition, a third band of Compound **1** at 258 nm attributed to n-p* transitions of the nitro substituent is observed.

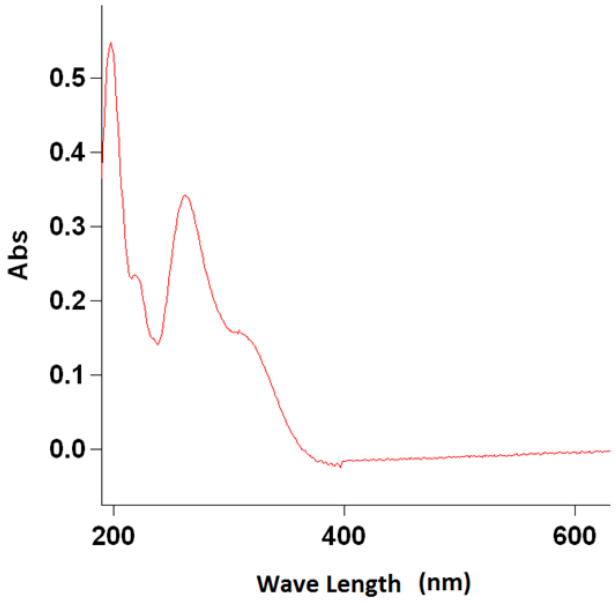

Figure 8. Absorption spectra of (*E*)-N-benzylidenaniline (**Compound 2**) in ACN.

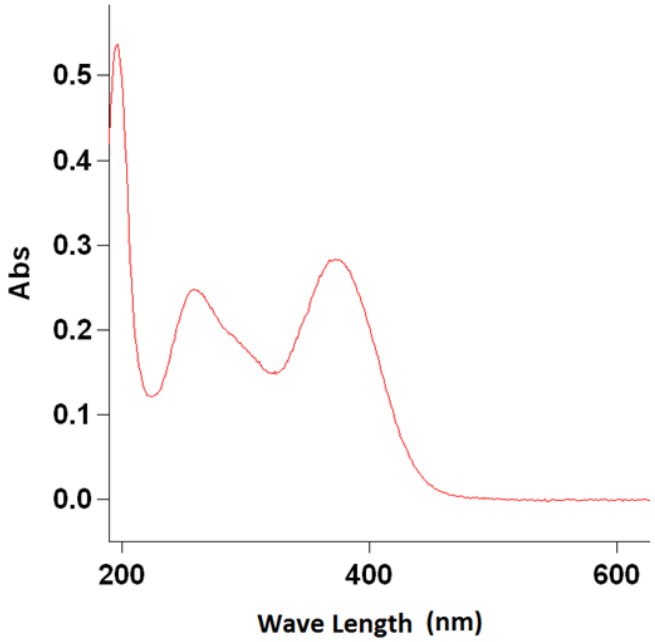

Figure 9. Absorption spectra of (*E*)-4-(4-nitrobenzyliden)amino)phenol (**Compound 1**) in ACN.

3.4. In vitro cytotoxicic assay

The *in vitro* cytotoxic assay showed that Compound **1** has a cytotoxic effect against human lymphoblastic leukemia MOLT-4 cells (Fig. 10). Compound **1** exhibits cytotoxic activity at 0.5 ppm and higher concentrations. At 0.5 ppm, Compound **1** eliminates 11.5% of cell population; at 20 ppm it

eliminates 100% of cells within 24 h. Some morphological changes such as nuclei swelling and cytoplasm disturbance were observed in surviving cells.

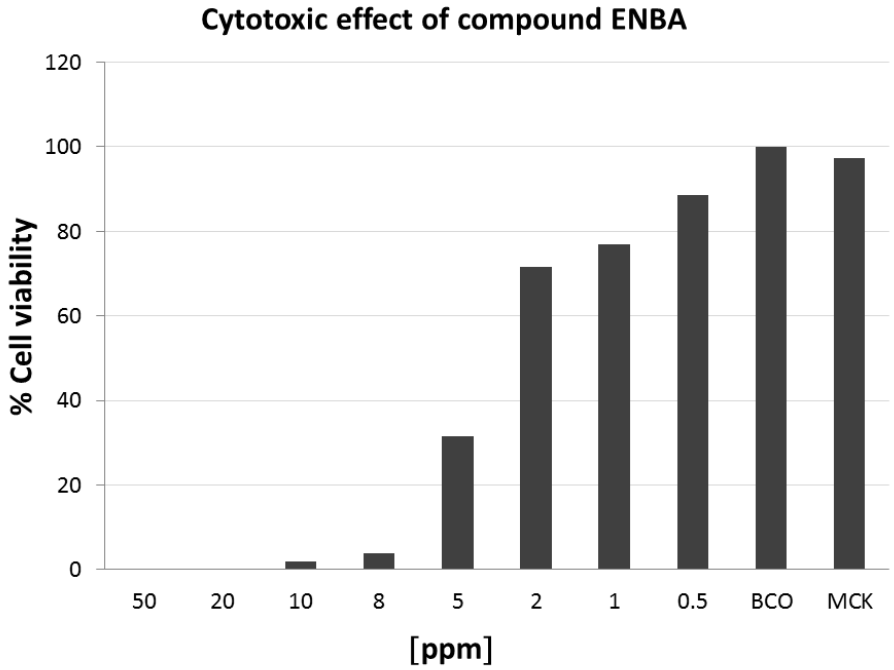

Figure 10. Cytotoxic effect of Compound **1** (ENBA) on lymphoblastic leukemia MOLT-4 cells. MCK is the mock culture.

3.5. Antibacterial assays

Compound **1** exhibited significant antibacterial activity against the gram-negative bacteria *Salmonella typhimurium*. Radial diffusion assays showed clear non-growth halos on agar surfaces in contact with Compound **1**. No significant differences were observed among 50 and 100 ppm (Fig. 11).

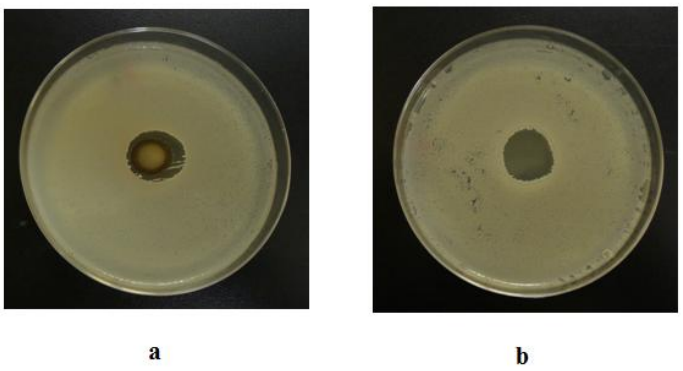

Figure 11. Effect of Compound **1** on gram-negative bacteria *Salmonella typhimurium* (a) 100 ppm, (b) 50 ppm.

3.6. Antifungal assays

Fig.12 shows that *Penicillium sp.* is more sensitive to the presence of Compound **1** than *Aspergillus niger*. Sporulation of *Penicillium sp.* is totally absent at 125 ppm and appears to be unusual at the well corresponding to 50 ppm. Similar results were obtained for the assay with *A. niger*, where the characteristic black color of sporulation is almost absent at 125 ppm and completely absent at 250 ppm. According to these results, Compound **1** has very promising potential as cytotoxic, antibacterial and antifungal agent, which opens a path for future research.

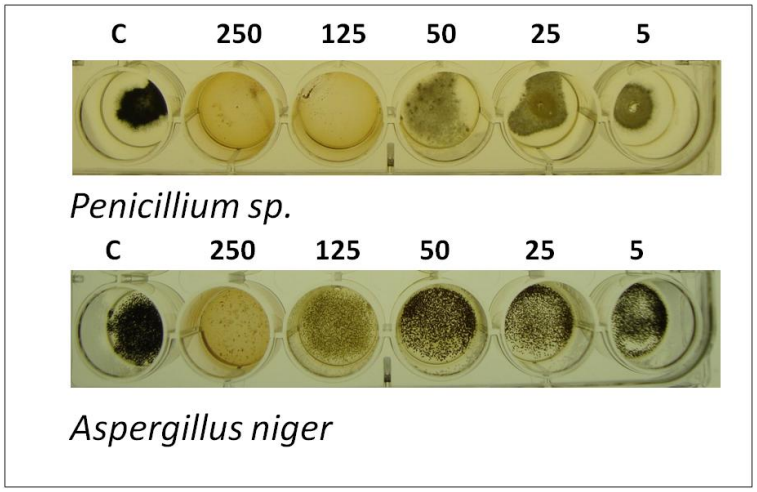

Figure 12. Effect of Compound **1** on filamentous fungus growing inhibition.

4. CONCLUSIONS

In summary, the crystal structure of the Schiff base shows *trans*-configuration with respect to the C=N double bond; this configuration is consistent with previous work in our group (*vide supra*). The intermolecular interaction and the co-crystallization of ethanol seem to be reliable to obtain suitable monocrystals. The electrochemical study of Compound **1** reveals the presence of two reduction processes associated to the anion and dianion radical formation. Comparison of the electrochemical characterization of Compounds **2** and **1** showed that these two reduction processes can be associated to the activity of the imine group. The dianion radical formation potential is slightly different from that obtained for Compound **2** because of the effect of substituent groups. The effect of the OH^- and NO_2 substituent groups in Compound **1** causes a shift to more positive potentials than those obtained for the Compound **2**. According to biological activity studies, the Compound **1** has potential as cytotoxic, antibacterial and antifungal agent.

ACKNOWLEDGMENTS
The authors thank CONACYT (Grant 156450) and also the Chemistry Faculty of the Autonomous University of Nuevo León for funding this project, Thanks to Dr. Rosa Santillán for performing the X-ray diffraction. In addition, Rodrigo Chan Navarro thanks CONACYT for the scholarship.

Appendix A. Supplementary data:

CCDC 976896 contains the supplementary crystallographic data for the organotin compound. These data can be obtained free of charge at http://www.ccdc.cam.ac.uk/conts/retrieving.html, or from the Cambridge Crystallographic Data Centre, 12 Union Road, Cambridge CB2 1EZ, UK; fax: (+44) 1223-336-033; e-mail: deposit@ccdc.cam.ac.uk.

References

1. G. Valli, K. Ramu, P. Mareeswari, A. T. Thirupathi, *J. Pharm. Res*. 5 (2012) 3453.
2. S.E. Harptrite, S.D. Collins, A. Oksman, D.E. Goldberg, V. Sharma, *Med. Chem*. 4 (2008) 392.
3. K. Sztanke, A. Maziarka, A. Osinka, M. Sztanke Bioorg. *Med Chem.* 21 (2013) 3648.
4. K.S. Kumar, S. Ganguly, R. Veerasamy, E. De Clercg, *Eur. J. Med. Chem.* 45 (2010) 5474.
5. S. Ren, R. Wang, K. Komatsu, P. Bonaz-Krause, Y. Zyrianov, C.E. McKenna, C. Csipke, Z.A. Tokes, E.J. Lien, *J. Med. Chem*. 45 (2002) 410.
6. M.S. Alam, J.H. Choi, D.U. Lee, *Bioorg. Med. Chem*. 20 (2012) 4103.
7. H.J. Zhang, X. Qin, K. Liu, D.D. Zhu, X.M. Wang, H.L. Zhu , *Bioorg. Med. Chem.* 19 (2011) 5708.
8. P. Przybylski, A. Huczynski, K. Pyta, B. Brzezinski, F. Bartl, *Curr. Org. Chem.* 13, (2009) 124.
9. W. Chen, W. Ou,L. Wang, Y. Hao, J. Cheng, J. Li, Y. N.Liu, *Dalton Trans* 42 (2013) 15678.
10. L.-X. Cheng, J.-J. Tang, H. Luo, X.-L. Jin, F. Dai, J. Yang, Y.-P. Qian, X.-Z. Li and B. Zhou, Bioorg. *Med. Chem. Lett.* 20 (2010) 2417.
11. V.M. Jiménez-Pérez, M. Ibarra, B.M. Muñoz-Flores, A. Gómez, R. Santillán, E. Hernández, S. Bernès, N. Waksman, R. Ramírez, *J. Mol. Struct.* 1031 (2013) 168.
12. V.M. Jiménez-Pérez, B.M. Muñoz-Flores, A. Gómez, B.I. Kharisov, R. Santillán, M. E. Ochoa, L.M. Blanco Jerez, C. García, N. Waksman, R. Ramírez, *J. Mol. Struct.* 1058 (2014) 9.
13. M.J. Carter, D.P. Rillema, F. Basolo, *J. Am. Chem. Soc.* 96 (1974) 392.
14. [D.F. Averill, R.F. Broman, *Inorg. Chem*. 17 (1978) 3389.
15. G.M. Sheldrick, SHELX97, Programs for Crystal Structure Solution and Refinement, University of Göttingen, Göttingen, 1997.
16. L.J. Farrugia, *J. Appl. Crystallogr.* 32 (1999) 837.
17. ORTEP 3 L.J. Farrugia, *J. Appl. Crystallogr.* 30 (1997) 837.
18. M.B. Murphy-Jolly, S.B. Owens Jr, J.L. Freeman, G.M. Gray, C.M. Lawson, D.P. Shelton, *Eur. J. Inorg. Chem.* 33 (2010) 5263.
19. B.M. Muñoz-Flores, R. Santillán, M. Rodríguez, J.M. Méndez, M. Romero, N. Farfán, P.G. Lacroix, K. Nakatani, G. Ramos-Ortíz, J.L. Maldonado, *J. Organomet. Chem*. 693 (2008) 1321.
20. B.M. Muñoz-Flores, V.M. Jiménez-Pérez, R. Santillan, M.E. Ochoa, N. Waksman, *Acta Cryst*. Sect: E68 (2012) o175.
21. C.F. Macrae, I.J. Bruno, J.A. Chisholm, P.R. Edgington, P. McCabe, E. Pidcock, L. Rodriguez-Monge, R. Taylor, J. van de Streek, P.A.Wood, *J. Appl. Cryst*. 41 (2008) 466.
22. E.N. Aguilera, L.M. Blanco, A.M. Huerta, L.A. Obregón, *Port. Electrochim. Acta*, 27 (2009) 317-328.
23. J.R. Irigoyen, L.M. Blanco, S.T. López, *Int. J. Electrochem. Sci*., 7 (2012) 11246-11256.
24. E.N. Aguilera, L.M. Blanco, J. Alonso, *Electrochim. Acta* 98 (2013) 82-87.